
Michelson-Interferometer (INT)

ANFANGERPRAKTIKUM TEIL III, PHYSIK DEPARTMENT,
TUM

BERKE MERT
Matr. 03738893

JEDD PAGE
Matr. 03746102

03. July 2023

Contents

1	Introduction	2
2	Theoretical foundation	2
2.1	Dual-beam interference	2
2.2	Michelson interferometer	3
2.3	Pressure-dependent refraction index of gases	4
2.4	Refraction index of transparent solid bodies	4
3	Experimental procedure	4
4	Evaluation & results	5
4.1	Determining the pitch of the adjustment screw	5
4.2	Calculating air's refraction index	6
4.3	Calculating the refraction index of a Plexiglas plate	6
5	Error analysis	7
5.1	Weighted arithmetic mean	7
5.2	Gaussian Error Propagation	8
6	Literature	8

1 Introduction

The luminiferous aether was the postulated medium for the propagation of light. It was used to explain the propagation of electromagnetic waves to propagate through vacuum, something that waves unimaginable in the past.

The Aether theory, was later disproven by Albert A. Michelson and Edward W. Morley in the so-called Michelson-Morley-Interferometry experiment, which is used in this experiment to calculate the optical path length of a shiftable mirror, and the refraction indices of air and Plexiglas.

2 Theoretical foundation

2.1 Dual-beam interference

An electromagnetic wave can be described in time and space through an electric field, $\vec{E}(\vec{r}, t)$. The form of the electromagnetic wave can be simplified, if it's assumed that it is a monochromatic wave propagating along a fixed point on the z-axis,

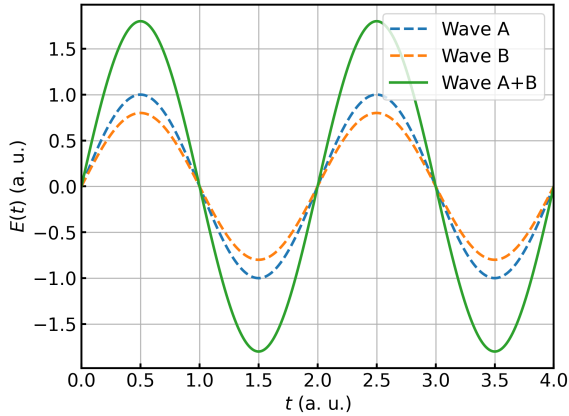
$$E(t) = E_0 \exp\{i(\omega t + \Phi)\}, \quad (1)$$

where $\omega = 2\pi\nu$ is the angular frequency of the wave, Φ is a constant phase-shift of the wave.

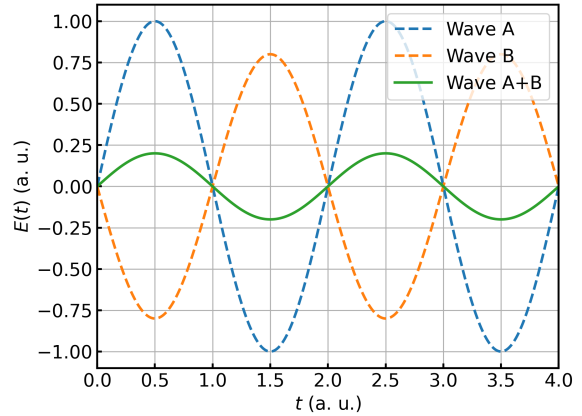
If two waves overlap the resulting wave is a superposition of the two of two,

$$E(t) = E_{0,1} \exp\{i(\omega t + \Phi_1)\} + E_{0,2} \exp\{i(\omega t + \Phi_2)\}. \quad (2)$$

Figure 1a and 1b show the superposition of two arbitrary waves with a phase-shift difference $\Delta\Phi = \Phi_2 - \Phi_1$ of 0 and π .



(a) Phase-shift difference $\Delta\Phi = 0$



(b) Phase-shift difference $\Delta\Phi = \pi$

Figure 1: Superposition of the real component of two electromagnetic waves with exemplary phase-shift difference.

The time-dependent electric field of the visible light spectrum oscillates with a frequency of about 10^{14} Hz and is therefore not observable. In experiments, the time-average of the electric field or the so-called

Intensity of the wave, I , is measured according to,

$$I = \langle E(t) \rangle_t = E(t) \cdot E^*(t) = I_1 + I_2 + 2\sqrt{I_1 I_2} \cos(\Delta\Phi). \quad (3)$$

From equation 3, it can be seen that the intensity has a minimum/maximum of order N at

$$\Delta\Phi = \begin{cases} 2\pi N & \text{for maxima,} \\ 2\pi (N + \frac{1}{2}) & \text{for minima.} \end{cases} \quad (4)$$

When a wave propagates through space, it travels the optical path length which is defined as follows,

$$s = l \cdot n, \quad (5)$$

where l is the distance of the path in a vacuum and n is the refraction index. The difference between the optical path lengths can then be determined with,

$$\Delta s = \Delta\Phi \frac{\lambda}{2\pi}. \quad (6)$$

The interference conditions therefor change to,

$$\Delta s = \begin{cases} N\lambda & \text{for maxima,} \\ (N + \frac{1}{2})\lambda & \text{for minima.} \end{cases} \quad (7)$$

2.2 Michelson interferometer

Figure 2 shows a schematic construction of a Michelson interferometer, where laser light (coherent light source) is divided into two partial beams at a half-silvered mirror M . The resulting two beams are then reflected with the mirrors $M1$ and $M2$ and then recombined at the M to create the desired interference patterns on the detector E .

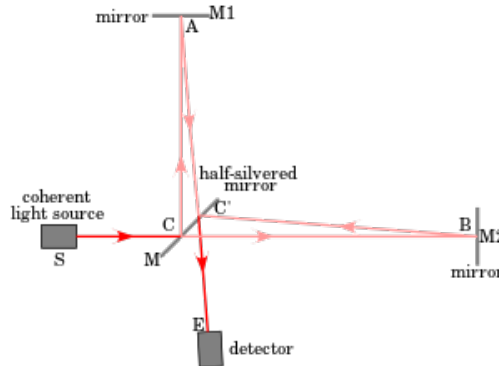


Figure 2: Schematic construction of a Michelson interferometer.

The difference of the optical path length of the two partial beams is therefore determined by the difference of the difference of the geometrical path length or the change of the refraction medium,

$$\Delta s = 2 \cdot \Delta l \cdot n, \text{ or} \quad (8)$$

$$\Delta s = 2 \cdot l \cdot \Delta n, \quad (9)$$

with the factor 2 taking into account the forward and back path of the partial beams.

2.3 Pressure-dependent refraction index of gases

As equation 9 shows, the interference pattern on the detector screen can be dependent on the refraction index of the different media. The refraction index itself is dependent on the interaction of electromagnetic waves with the electrons in a medium, and is therefore strongly dependent on the electron density in the medium. This means the refraction index of a gaseous medium can be varied by compressing the gas and thereby increasing the gas density in the medium.

Assuming ideal gas conditions and a linear relation between the gas density and the refraction index, it can be derived that,

$$n = 1 + \chi \cdot \frac{p}{T}, \quad (10)$$

where χ is a proportionality constant, p is the pressure in the gas, and T is the temperature of the gas.

2.4 Refraction index of transparent solid bodies

It is not practical to change the density of the body by compression, but the interference pattern can be changed by rotating the body, which changes the geometric path of the partial beams. Figure 3 shows the change of the optical path length after rotating the body.

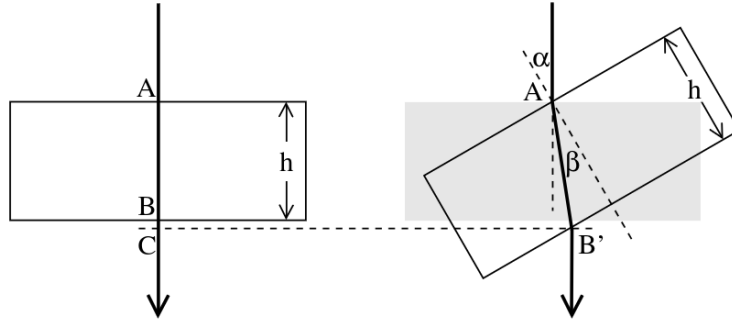


Figure 3: Propagation of a light beam perpendicular to the boundary surface of a solid medium on the left, and the light beam hitting the boundary surface at a slight angle α on the right. The solid body has the width h , the refraction index n and is in air ($n_{air} \approx 1$).

Using trigonometric identities and Snellius' refraction law, it can be shown that the difference of the optical path lengths of two partial light beams is given by,

$$\Delta s = 2 \cdot h \left(1 - n - \cos \alpha + \sqrt{n^2 - \sin^2 \alpha} \right), \quad (11)$$

where h is the width and n is the refraction index of the cuboid.

3 Experimental procedure

The setup of the experiment can be seen in figure 4. A Michelson-interferometer is used in conjunction with a helium neon laser with a wavelength of 633nm. Care has to be taken, when adjusting the beam path, as the slight adjustments of the mirror, have a large impact on the beam. To adjust the beam, it is best to start at the first mirror, make sure the reflected beam is pointing directly to the centre of the next mirror before moving on. Once all the mirrors are adjusted a interference pattern should be seen on the screen.

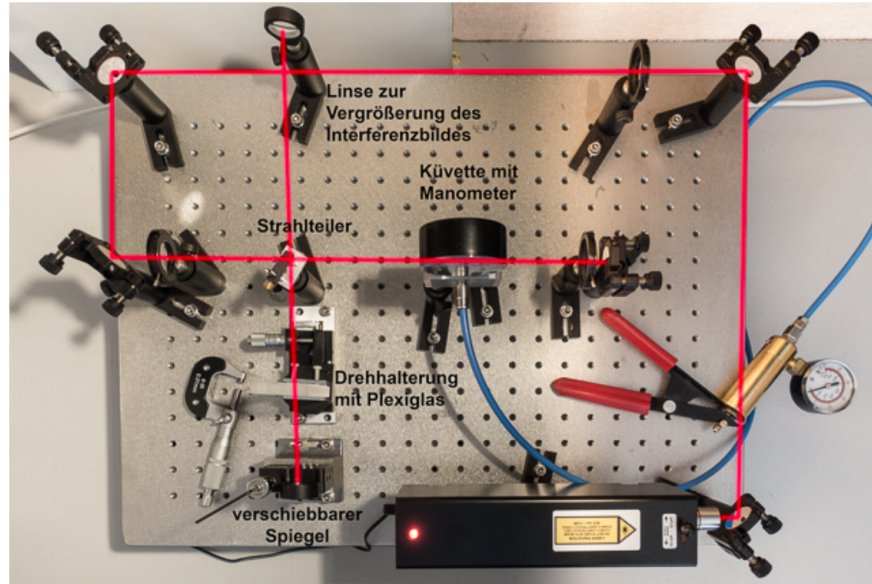


Figure 4: The experimental setup of the Michelson-interferometer, including the vacuum pump and the Plexiglas plate.

The first part of the experiment, determining the pitch of the adjusting screw on the mirror this setup is used. To calculate the pitch d and thereby the displacement of the mirror for one screw rotation, the adjusting screw is turned slowly and the interference maxima are counted. One hundred maxima are counted and then the position of the screw is noted. This measurement is repeated four times.

For the next part of the experiment we determine the pressure dependence of the refraction index of air. This is done, by inserting a cylindrical vacuum chamber with Plexiglas lids in the beam-line between the adjustable mirror and the screen. The vacuum chamber is $50 \pm 0.5\text{mm}$ long and has both a manometer and a hand pump attached. Using the hand pump air is slowly pumped out of the vacuum chamber, a change in the refraction index is made observable through a change in the interference pattern. For every 3rd maxima observed a pressure reading is made. The measurement is then repeated a second time.

The last measurement of the experiment concerns the refraction index of a $5 \pm 0.5\text{mm}$ thick Plexiglas plate. This is done by varying the incidence of the laser beam on the Plexiglas plate. The Plexiglas plate, placed in a turntable in the beam-line in front of the screen, is rotated via a micrometer in the turntable. From an incidence of 0° the Plexiglas is rotated in both directions. Once again the micrometer position is noted for every third maxima seen on the screen.

4 Evaluation & results

4.1 Determining the pitch of the adjustment screw

To evaluate the collected data, first we calculate the expected phase shift necessary to create one hundred maxima. We do this using equation 7 and get $\Delta S = 63.3 \pm 3.2\mu\text{m}$. Thereafter we calculate the displacement

of the screw for one full rotation, which equates to the screw's pitch. This is done with the equation.

$$d = \frac{\Delta S}{2} \cdot \frac{50}{m} \quad (12)$$

Where d is the screw's pitch, m is the number of lines measured for one hundred maxima and the factor $1/2$ accounts for the double beam. The calculation is repeated for all data sets and then the results is averaged. Giving us the final result of $d = 46.0 \pm 1.2 \mu\text{m}$. Which is a realistic result for a screw's pitch.

4.2 Calculating air's refraction index

The refraction index of air is determined using the data from the vacuum chamber. We can calculate the change in refraction index Δn from the raw data using equations 7 and 6, getting the relation

$$\Delta n = \frac{N \cdot \lambda}{2 \cdot l_{chamber}} \quad (13)$$

Fitting a linear function to the data Δp against Δn we get the slope $m = 0.261 \cdot 10^{-3}$. The slope correlates to the refraction index through equation 10 giving us the refraction index of air, $n_{air} = 1.000265 \pm 0$. Comparing this value to the literature value of 1.000293 [1] the experimental value is close to the theoretical value and off by only a small margin. The fit function and the data points can be seen in figure 5.

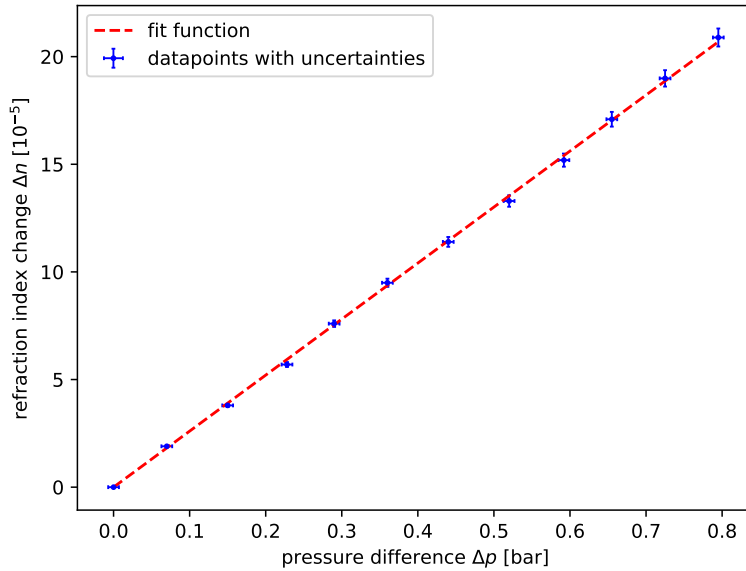


Figure 5: The relation of the change in refractive index against the pressure change.

4.3 Calculating the refraction index of a Plexiglas plate

Lastly, the refraction index of a Plexiglas plate is calculated and the result is evaluated. The method mentioned in the previous section gives as the displacement of the micrometer and the order of the maxima as raw data. First, we can calculate the angle of incidence of the Plexiglas plate using the measured displacement

of the micrometer. This is done using the small angle approximation and the lever-arm $d = 28 \pm 1$ of the turntable onto which the plate is mounted. This gives us

$$\Theta = \frac{x}{d} \quad (14)$$

where x is the displacement of the micrometer. Now, with a fit function, derived from equations 7 and 3 of the form

$$N(\Theta) = \frac{2h}{\lambda \cdot (1 - n - \cos \Theta + \sqrt{n^2 - \sin^2 \Theta})} \quad (15)$$

with n as the fit parameter and $h = 5.0 \pm 0.1$ as the thickness of the Plexiglas plate. In our equation n represents the refraction index of the medium, in our case Plexiglas. From the fitted function we obtain the value $n = 1.001$, which compared to the literature value of 1.495 [2] is incorrect. The cause of this discrepancy is not certain, however is with large probability due to bad measurements. The fitted function fits well with the measured data. The results of the fitted function and the measured data can be seen in figure 6.

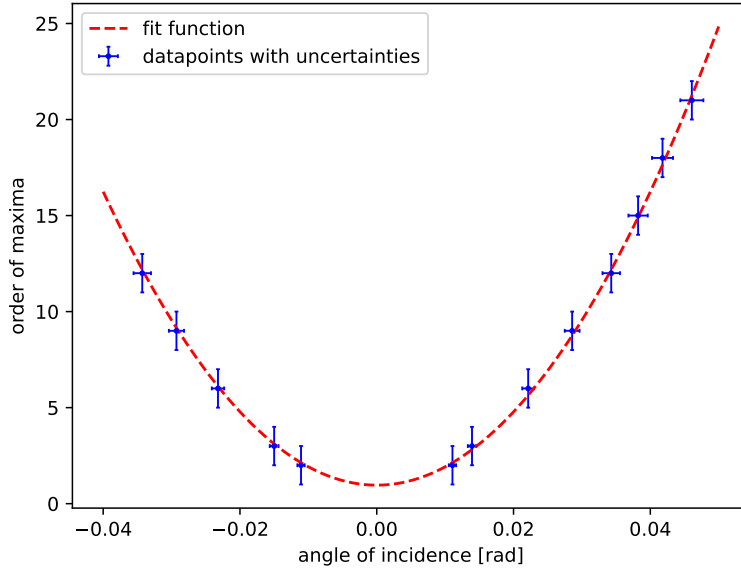


Figure 6: The relation of the order of maxima against the angle of incidence.

5 Error analysis

5.1 Weighted arithmetic mean

To find the mean of multiple values, that have different uncertainties, the weighted arithmetic mean

$$\frac{\sum_{i=1}^n w_i \cdot x_i}{\sum_{i=1}^n w_i} \quad (16)$$

was used, where w_i are the weights of the different data elements and are given by

$$w_i = \frac{1}{u^2(x_i)}. \quad (17)$$

$u(x_i)$ describe the errors of the different values. To find the uncertainty of the weighted mean, the inner and outer uncertainties are compared. The inner uncertainty is given by

$$u_{int}(\bar{x}) = \sqrt{\frac{1}{\sum_{i=1}^n w_i}} \quad (18)$$

and the outer uncertainty by

$$u_{ext}(\bar{x}) = \sqrt{\frac{\sum_{i=1}^n (w_i \cdot (x_i - \bar{x})^2)}{(n-1) \cdot \sum_{i=1}^n w_i}}. \quad (19)$$

Of the two found uncertainties, the bigger one is used [3].

5.2 Gaussian Error Propagation

For calculations using experimental values with uncertainties the Gaussian formula for error propagation

$$u(\bar{g}) = \sqrt{\sum_{i=1}^N \left(\frac{\partial g}{\partial x_i} \right)^2 u^2(\bar{x}_i)}, \quad (20)$$

was used [3].

6 Literature

References

- [1] Faughn Jerry S. Serway Raymond. *The Law of Refraction. College Physics. Sixth edition.* Brooks/Cole-Thomson Learning, 2003.
- [2] Glenn Eret. The physics hypertextbook, refraction. <https://physics.info/refraction/>, 2023. last visited 03.07.2023.
- [3] Physics department TUM. Hinweise zur Beurteilung von Messungen, Messergebnissen und Messunsicherheiten (ABW). <https://www.ph.tum.de/academics/org/labs/ap/org/ABW.pdf>, 20xx. last visited 5.5.2021.